



Published in final edited form as:

Inorg Chem. 2013 March 18; 52(6): 2933–2938. doi:10.1021/ic302327p.

Preparation of Primary Amine Derivatives of the Magic-Size Nanocluster (CdSe)₁₃

Yuanyuan Wang[†], Yi Hsin Liu[†], Ying Zhang[†], Paul J. Kowalski[‡], Henry W. Rohrs[†], and William E. Buhro^{†,*}

[†]Department of Chemistry, Washington University, St. Louis, Missouri 63130-4899.

[‡]Bruker Daltonics, Inc. 40 Manning Road, Billerica, MA 01821 (USA)

Abstract

Four [(CdSe)₁₃(RNH₂)₁₃] derivatives (R = *n*-propyl, *n*-pentyl, *n*-octyl, and oleyl) are prepared by reaction of Cd(OAc)₂·2H₂O and selenourea in the corresponding primary-amine solvent. The nanoclusters grow in spontaneously formed amine-bilayer templates, and are characterized by elemental analysis, IR spectroscopy, UV-visible spectroscopy, TEM, and low-angle XRD. The derivative [(CdSe)₁₃(*n*-propylamine)₁₃] is isolated as a yellowish-white solid (MP 98 °C) on the gram scale. These compounds are the first derivatives of magic-size CdSe nanoclusters to be isolated in purity.

Introduction

Discretely sized semiconductor nanoclusters have been spectroscopically detected since the early work of Henglein and coworkers,¹ and have been observed as intermediates in the growth of larger colloidal nanocrystals.^{2–4} Nanoclusters of CdSe have been of intense experimental^{5–8} and theoretical^{9–11} interest since their mass-spectrometric characterization by Kasuya and coworkers in 2004.¹² Among these so-called magic-size nanoclusters (CdSe)₁₃, (CdSe)₁₉, (CdSe)₃₃, and (CdSe)₃₄ have been most studied. Until recently,¹³ magic-size CdSe nanoclusters had been prepared only in mixtures of various sizes,^{5,8,14} and no single, discrete-size nanocluster had been isolated in purity.

Our interest in magic-size CdSe nanoclusters began when we observed them as reaction intermediates in the low-temperature synthesis of wurtzitic CdSe nanoribbons or quantum belts.^{15,16} In the course of our initial work, we isolated pure [(CdSe)₁₃(*n*-octylamine)₁₃] and [(CdSe)₁₃(oleylamine)₁₃].¹³ As such compounds now appear to be useful nanocrystal synthons,^{15,16} we sought to prepare a suitable derivative in gram quantities.

We now report full details of the synthesis and characterization of four primary amine derivatives of (CdSe)₁₃, each having the stoichiometry [(CdSe)₁₃(RNH₂)₁₃]. We show that each result from a templated synthesis in which the nanoclusters grow within amine-bilayer mesophases. The [(CdSe)₁₃(*n*-propylamine)₁₃] derivative is conveniently prepared on the gram scale. We hope that access to preparative quantities of (CdSe)₁₃ will promote further experimental studies of its structure, reactivity, physical properties, and use as a nanocrystal precursor.

* To whom correspondence should be addressed. buhro@wustl.edu.

Experimental Section

Materials

n-Propylamine (+98%), *n*-pentylamine (+99%), *n*-octylamine (+99%), oleylamine (technical grade, 70%), Cd(OAc)₂·2H₂O and trioctylphosphine (TOP, 97%) were purchased from Aldrich, and selenourea (99.9%, metal basis) from Alpha Aesar. All were used as received and stored under N₂. Toluene from Sigma-Aldrich (CHROMASOLV®, for HPLC, ≥ 99.9%) was purged with dry N₂ for at least 1 h and stored under N₂ prior to use.

Analyses

Elemental analyses (C, H, N) were obtained from Galbraith Laboratories, Inc. (Knoxville, TN). UV-visible spectra were obtained from a Perkin Lambda 950 UV/Vis spectrometer. IR spectra were obtained from a Perkin Elmer Spectrum BX FT-IR System. The XRD patterns were obtained from a Rigaku Dmax A vertical powder diffractometer with Cu K α radiation ($\lambda=1.5418 \text{ \AA}$). Low-resolution TEM images were obtained from a JEOL 2000FX microscope operating at 200 KV. The melting point was obtained on a Mel-temp II Laboratory Device. The analysis by Rutherford backscattering spectrometry (RBS) was provided by the Characterization Facility at the University of Minnesota (Minneapolis, MN). The LDI mass spectra were recorded on a Bruker ultrafleXtreme MALDI-TOF/TOF mass spectrometer. No matrix was employed in these mass-spectral analyses.

Preparation of [(CdSe)₁₃(*n*-propylamine)₁₃]

All synthetic procedures were conducted under N₂. In a large-scale synthesis, Cd(OAc)₂·2H₂O (1.30 g, 4.80 mmol) was dissolved in *n*-propylamine (40.0 g, 0.681 mol) in a septum-capped schlenk tube, heated in a 50 °C oil bath for 1 h, and allowed to cool to room temperature. Selenourea (1.0 g, 8.2 mmol) was added in *n*-propylamine (10.0 g, 0.170 mol) in the glove box, and then sonicated in a bench-top sonicator for dissolution.

The selenourea solution was injected into cadmium-precursor solution at room temperature (20-25 °C) without stirring. The color of the reaction mixture changed immediately after injection from colorless (0 min) to light-yellow (viscous, 5 s), yellow (cloudy with a white precipitate, 1 min) and red (cloudy with a white precipitate, 1 h). After another 2 h under N₂ without stirring, (CdSe)₁₃ was deposited as reddish-white precipitate under a light-red supernatant.

The reaction mixture was subsequently heated at 50 °C in an oil bath for 40 min, during which the mixture turned a darker shade of red, with a white precipitate. The red solution contained elemental selenium as the colored byproduct, which was removed by addition of TOP (1.3 g) to form TOP=Se, resulting in a colorless solution with a white precipitate.

The white precipitate was separated using a bench-top centrifuge (700 g, 30 s), and the colorless supernatant was discarded. The remaining white slush was combined with a propylamine solution (20 mL, 20% w/w in toluene), and the mixture was recentrifuged and the supernatant discarded. This purification process was repeated 5 times in total. The residual solvent was removed in vacuo, leaving [(CdSe)₁₃(*n*-propylamine)₁₃] as a yellowish-white solid (1.19 g, 0.365 mmol, 97.5%).

Smaller-scale syntheses were conducted similarly, typically using Cd(OAc)₂·2H₂O (65 mg, 0.24 mmol) in *n*-propylamine (5.7 g, 0.097 mol), and selenourea (50 mg, 0.41 mmol) in *n*-propylamine (1.2 g, 9.3 mmol). The elemental-selenium byproduct was removed with added TOP (65 mg). The product precipitate was purified with a propylamine solution (5 × 5 mL,

20% w/w in toluene) as described above, leaving [(CdSe)₁₃(*n*-propylamine)₁₃] as a yellowish-white solid (59.3 mg, 0.018 mmol, 97.1%).

Characterization: MP (98 ± 2 °C). IR (KBr, cm⁻¹, 25 °C): 3346 (w, NH stretch), 3245 (sh, NH stretch), 3202 (m), 3122 (m), 2953 (m), 2921 (s), 2869 (m), 2851 (m), 1646 (s, NH₂ deformation), 1559 (s, NH₂ deformation), 1458 (w), 1404 (s), 1351 (w), 1032 (w), 1007 (m), 965 (w) (Figure 1). UV-Vis (toluene) λ_{max}, nm: 334, 349 (Figure 2). Anal Calcd for [(CdSe)₁₃(*n*-propylamine)₁₃]: C, 14.37; H, 3.59; N, 5.59. Found, C, 14.80; H, 3.46; N, 5.51. All values are given as percentages.

Preparation of [(CdSe)₁₃(*n*-pentylamine)₁₃]

All synthetic procedures were conducted under the same general conditions for the [(CdSe)₁₃(*n*-propylamine)₁₃] preparation, except for the reaction solvent. Cd(OAc)₂·2H₂O (65 mg, 0.24 mmol) was dissolved in *n*-pentylamine (5.7 g, 0.066 mol), heated in a 70 °C oil bath for one hour, and allowed to cool to room temperature. Selenourea (50 mg, 0.41 mmol) was dissolved in *n*-pentylamine (1.2 g, 0.013 mol).

After injecting the selenourea solution into the Cd(OAc)₂ solution at room temperature without stirring, the reaction mixture turned from colorless (0 min) to green yellow (1 min), light yellow (cloudy, 5 min), and yellow (cloudy with a white precipitate, 15 min), and light red (cloudy with a white precipitate, 2 h). After another 5 h, a white precipitate formed under a red supernatant. The mixture was heated at 70 °C for 40 min. TOP (65 mg) was injected to remove the elemental-selenium byproduct. The remaining white precipitate was separated from the colorless supernatant using a purification process described above, but with *n*-pentylamine solution (5 × 5 mL, 20% w/w in toluene). The residual solvent was removed in vacuo, leaving [(CdSe)₁₃(*n*-pentylamine)₁₃] as a slushy white solid (62.9 mg, 0.017 mmol, 92.6%). To ensure removal of the last traces of *n*-pentylamine for elemental analysis, pure toluene (5 × 5 mL) was used in the purification steps.

Characterization: IR (KBr, cm⁻¹, 25 °C): 3368 (w, NH stretch), 3238 (sh, NH stretch), 3205 (m), 3128 (m), 2953 (w), 2920 (s), 2868 (sh), 2849 (s), 1577 (s, NH₂ deformation), 1458 (w), 1352 (w), 1031 (w), 1007 (w), 969 (w) (Figure 1). All values are given as percentages. UV-Vis (toluene) λ_{max}, nm: 337, 351 (Figure 2). Anal Calcd for [(CdSe)₁₃(*n*-pentylamine)₁₃]: C, 21.54; H, 4.67; N, 5.02. Found, C, 21.44; H, 4.42; N, 4.82.

Preparation of [(CdSe)₁₃(*n*-octylamine)₁₃]

All synthetic procedures were conducted under the same general conditions for the [(CdSe)₁₃(*n*-propylamine)₁₃] synthesis, except for the reaction solvent. Cd(OAc)₂·2H₂O was dissolved in *n*-octylamine (5.7 g, 0.044 mol), heated in a 70 °C oil bath for one hour, and allowed to cool to room temperature. Selenourea was dissolved in *n*-octylamine (1.2 g, 0.0093 mol).

After injecting selenourea solution into the Cd(OAc)₂ solution at room temperature, the reaction mixture turned from colorless (0 min) to green yellow (1 min), white yellow (cloudy, 5 min), yellow (cloudy, 15 min), and light red (cloudy, 2 h). After another 5-10 h, a white precipitate formed under a red supernatant. The reaction mixture was subsequently heated at 70 °C in an oil bath for 40 min. TOP (65 mg) was injected to remove elemental-selenium byproduct. The purification procedure was the same as that used in the synthesis [(CdSe)₁₃(*n*-propylamine)₁₃], but with *n*-octylamine solution (5 × 5 mL, 20% w/w in toluene). The residual solvent was removed in vacuo, leaving [(CdSe)₁₃(*n*-octylamine)₁₃] as a white slushy solid (75 mg, 0.018 mmol, 95.9 %). To ensure removal of the last traces of *n*-octylamine for elemental analysis, pure toluene (5 × 5 mL) was used in the purification steps.

Characterization: IR (KBr, cm^{-1} , 25 °C): 3260 (w, NH stretch), 3234 (w, NH stretch), 3204 (w), 2952 (m), 2922 (vs), 2850 (vs), 1584 (s, NH_2 deformation), 1466 (s), 1376 (w), 1352 (w), 1165 (w), 1062 (w), 1026 (w), 972 (w) (Figure 1). UV-Vis (toluene) λ_{max} , nm: 311, 337, 349 (Figure 2). MS m/z (relative intensity): 6507.5149 ((CdSe)₃₄, 7.69%), 6318.0317 ((CdSe)₃₃, 5.38%), 3638.1176 ((CdSe)₁₉, 10.8%), 2488.5692 ((CdSe)₁₃, 100%).¹³ RBS: Cd:Se = 1.05:0.95.¹³ Anal Calcd for [(CdSe)₁₃(*n*-octylamine)₁₃]: C, 29.97; H, 5.97; N, 4.37. Found, C, 30.89; H, 5.84; N, 4.57.¹³ All values are given as percentages.

Preparation of [(CdSe)₁₃(oleylamine)₁₃]

All synthetic procedures were conducted under the same general conditions for the [(CdSe)₁₃(*n*-propylamine)₁₃] synthesis, except for the reaction solvent. Cd(OAc)₂·2H₂O was dissolved oleylamine (1.5 g, 5.6 mmol), heated in a 70 °C oil bath for one hour, and allowed to cool to room temperature. Selenourea was dissolved in oleylamine (6.8 g, 0.025 mol). The color changes much slower after injecting selenourea solution into the Cd(OAc)₂ solution at room temperature. It changes from colorless (0 min) to bright green-yellow (transparent, 30 sec), and orange (viscous, overnight), and orange-red (cloudy, over 20 h). After two days, a white-orange precipitate formed under a red supernatant. TOP (65 mg) was injected to remove byproduct elemental-selenium. The purification procedure was the same as that used in the synthesis [(CdSe)₁₃(*n*-propylamine)₁₃], but with oleylamine solution (5 × 5 mL, 20% w/w in toluene). The residual solvent was removed in vacuo, leaving [(CdSe)₁₃(oleylamine)₁₃] as a white slushy solid (97 mg, 0.016mmol, 86.6%). To ensure removal of the last traces of oleylamine for elemental analysis, pure toluene (5 × 5 mL) was used in the purification steps.

Characterization: IR (KBr, cm^{-1} , 25 °C): 3271 (w, NH stretch), 3242 (m, NH stretch), 3208(m), 2955 (m), 2918 (vs), 2849 (vs), 1596 (sh, NH_2 deformation), 1578 (m, NH_2 deformation), 1466 (s), 1355 (s), 1018 (w), 963 (w) (Figure 1). UV-Vis (toluene) λ_{max} , nm: 310, 338, 349 (Figure 2). Anal Calcd for [(CdSe)₁₃(*n*-oleylamine)₁₃]: C, 47.04; H, 8.06; N, 3.05. Found, C, 49.26; H, 8.84; N, 5.03. All values are given as percentages.

Results

We previously reported the room-temperature synthesis of [(CdSe)₁₃(*n*-octylamine)₁₃] by reaction of cadmium acetate (dihydrate) and selenourea in *n*-octylamine solvent.¹³ Reaction monitoring established the chemical pathway summarized in Scheme 1. The combination of cadmium acetate and *n*-octylamine resulted in the spontaneous formation of an amine-bilayer mesostructure¹⁷ in which bilayers of *n*-octylamine separated cadmium acetate layers. This lamellar mesostructure served as a template for the growth of (CdSe)₁₃ nanoclusters upon addition of selenourea. A mixture of magic-size CdSe nanoclusters was initially formed, including (CdSe)₁₃, (CdSe)₁₉, (CdSe)₃₃, and (CdSe)₃₄, which equilibrated exclusively to (CdSe)₁₃ over 5-7 h at room temperature.¹³ We previously suggested that (CdSe)₁₃ is thermodynamically the most stable magic size within the amine-bilayer mesophase.¹³

A white slushy solid isolated from the equilibrated mixture was shown to be [(CdSe)₁₃(*n*-octylamine)₁₃] by a combination of elemental analysis, UV-visible spectroscopy, mass spectrometry, and Rutherford backscattering spectrometry (showing a Cd:Se ratio of 1:1).¹³ Some have argued that mass-spectrometry evidence for magic-size-nanocluster mass distributions is questionable, because various specimens having apparently different distributions of magic-size nanoclusters appear to give very similar mass distributions.¹⁸ However, our reported mass spectrum for (CdSe)₁₃ was markedly different than those published previously,¹² especially in that (CdSe)₁₃ was the base peak, present in much greater intensity than the peaks for other (CdSe)_x species.¹³

The template mesostructure remained intact in the as-synthesized $[(\text{CdSe})_{13}(n\text{-octylamine})_{13}]$, with the $(\text{CdSe})_{13}$ nanoclusters entrained within. We found that individual sheets of aggregated $[(\text{CdSe})_{13}(n\text{-octylamine})_x(\text{oleylamine})_{13-x}]$ were exfoliated (Scheme 1) when the initially bundled template mesostructure was allowed to stand in oleylamine solution, during which partial ligand exchange occurred. Sonication of the sheet structures in oleylamine solution completed the ligand exchange, degraded the sheet aggregates, and released molecular $[(\text{CdSe})_{13}(\text{oleylamine})_{13}]$ nanoclusters into solution.¹³

In this study, additional primary-amine derivatives of $(\text{CdSe})_{13}$ were similarly prepared in the corresponding primary-amine solvent. The $[(\text{CdSe})_{13}(\text{RNH}_2)_{13}]$ nanoclusters were isolated as slushy solids except for $[(\text{CdSe})_{13}(n\text{-propylamine})_{13}]$, which was a yellowish-white solid having a melting point of 98 °C. Satisfactory elemental analyses were obtained for $[(\text{CdSe})_{13}(\text{RNH}_2)_{13}]$, R = *n*-propyl and *n*-pentyl. The elemental analysis for $[(\text{CdSe})_{13}(n\text{-octylamine})_{13}]$ was slightly high in C, and that for $[(\text{CdSe})_{13}(\text{oleylamine})_{13}]$ was significantly high in C, H, and N, reflecting our difficulty in successfully washing away the excess long-chain alkylamine (used as solvent) from these slushy solids. As expected, the IR spectra of the $[(\text{CdSe})_{13}(\text{RNH}_2)_{13}]$ compounds exhibited absorbances corresponding only to the primary amine ligands, with the characteristic NH stretches and NH₂ deformations¹⁹ clearly observed (Figure 1). The IR spectra of $\text{Cd}(\text{OAc})_2 \cdot 2\text{H}_2\text{O}$, *n*-octylamine, and $[(\text{CdSe})_{13}(n\text{-octylamine})_{13}]$ are compared in Figure S1 to establish that the observed absorbances of $[(\text{CdSe})_{13}(n\text{-octylamine})_{13}]$ are displaced from those of the acetate ligand.

Evidence for the $(\text{CdSe})_{13}$ stoichiometry of the as-synthesized nanoclusters was obtained by UV-visible spectroscopy (Figure 2). As we previously reported,¹³ $[(\text{CdSe})_{13}(n\text{-octylamine})_{13}]$ exhibited three absorbances (311, 337, and 349 nm), which closely approached the electronic spectrum of $(\text{CdSe})_{13}$ calculated theoretically (315, 330, and 345 nm).⁹ The spectra of all four primary-amine derivatives were closely similar (Figure 2a), with small differences in peak positions and widths (Figure 2b) likely induced by the amine ligands. (The 315-nm absorbances were not resolved in the spectra of $[(\text{CdSe})_{13}(n\text{-propylamine})_{13}]$ and $[(\text{CdSe})_{13}(n\text{-pentylamine})_{13}]$.) Small variations in peak positions and line shapes in the absorption spectra of CdSe nanoclusters upon changes in surface ligation have been attributed to small perturbations of surface or electronic structure,²⁰ which seems to have occurred here as well.

Three of the Figure-2 spectra featured long scattering tails to longer wavelength, as a result of the bundled nature of the as-synthesized materials. This scattering tail was absent in the spectrum of $[(\text{CdSe})_{13}(\text{oleylamine})_{13}]$, because exfoliation occurred readily upon solvent dispersion of this derivative for spectral analysis. Notably, absorbances at 363, 389, and 413 nm, previously assigned to $(\text{CdSe})_{19}$, $(\text{CdSe})_{33}$, and $(\text{CdSe})_{34}$,^{9,15} were absent from all four spectra, establishing the spectroscopic purity of the $[(\text{CdSe})_{13}(\text{RNH}_2)_{13}]$ nanoclusters.

The bundled and exfoliated template features were determined by TEM imaging (Figure 3). Figure 3a shows bundled aggregates of $[(\text{CdSe})_{13}(n\text{-octylamine})_{13}]$,^{13,15}. The arrows indicate regions in which parallel stripes may be observed, constituting side views of the lamellar template depicted in Scheme 1. Exfoliation of individual layers from the lamellar mesophases as described above produced images like that in Figure 3b, in which triangular sheet-like aggregates of $[(\text{CdSe})_{13}(n\text{-octylamine})_x(\text{oleylamine})_{13-x}]$ were separated from the bundled templates. The zebra-stripe pattern evident in Figure 3b revealed additional structural order within the individual sheets or layers.^{13,15}

Images of the bundled and unbundled aggregates of $[(\text{CdSe})_{13}(n\text{-propylamine})_{13}]$ and $[(\text{CdSe})_{13}(n\text{-pentylamine})_{13}]$ are shown in Figure 3c-f. The lamellar-stripe pattern was not observed in the bundled aggregates of these compounds (Figure 3c, e), suggesting them to

be less well-ordered than the bundled aggregates of $[(\text{CdSe})_{13}(n\text{-octylamine})_{13}]$ (Figure 3a). This observation was supported by low-angle XRD (see below). Exfoliation of these compounds produced individual triangular sheets, like those for $[(\text{CdSe})_{13}(n\text{-octylamine})_{13}]$ (Figure 3b), confirming the initial lamellar architectures.

The images of “bundled” and unbundled aggregates of $[(\text{CdSe})_{13}(\text{oleylamine})_{13}]$ (Figure 3g, h) contrasted with those of the other primary-amine derivatives. The most-prominent feature in images of the as-synthesized $[(\text{CdSe})_{13}(\text{oleylamine})_{13}]$ were rolled sheets resembling half-cylinders. Parallel-stripe patterns were observed in some regions of the images (see the arrow in Figure 3g), indicative of a bundled, lamellar architecture. We note that the bundled aggregates of $[(\text{CdSe})_{13}(\text{oleylamine})_{13}]$ are the most easily exfoliated, as addition of oleylamine to the other bundled $[(\text{CdSe})_{13}(\text{RNH}_2)_{13}]$ mesophases induces spontaneous exfoliation upon ligand exchange. We therefore surmise that solvent dispersion of the bundled $[(\text{CdSe})_{13}(\text{oleylamine})_{13}]$ material for TEM sample preparation resulted in extensive exfoliation, as confirmed by the Figure-3h image. Low-angle XRD evidence is provided below for the bundled, lamellar structure of the as-synthesized material.

The low-angle XRD patterns (Figure 4) of the bundled $[(\text{CdSe})_{13}(\text{RNH}_2)_{13}]$ mesophases provided strong confirmatory evidence for their lamellar structures. Each contained a series of basal, $00l$ reflections (Table 1) corresponding to the layered architectures. The peaks were sharpest for $[(\text{CdSe})_{13}(n\text{-octylamine})_{13}]$, showing it to be the most highly ordered mesophase.

The d spacings calculated from the XRD patterns gave the interlayer spacings in the four lamellar mesostructures, which are plotted versus the number of carbon atoms in the primary-amine ligands in Figure 5. The data gave the expected linear relationship,^{21,22} except for the oleylamine point, which departed from the line because of the double bond in the ligand's chain. The line should extrapolate approximately to the inter-amine-head-group spacing at the y intercept, which was 0.80 nm. This value is close to the theoretical diameter of the $(\text{CdSe})_{13}$ nanocluster (see the Discussion).¹⁰ The result indicated that one monolayer of $(\text{CdSe})_{13}$ nanoclusters was interspersed between the amine bilayers, represented as the planar features in Scheme 1, in the lamellar-template mesostructures.

Discussion

The results reported here establish that the four $[(\text{CdSe})_{13}(\text{RNH}_2)_{13}]$ derivatives ($R = n$ -propyl, n -pentyl, n -octyl, and oleyl) are accessible by a common synthetic method, are formed by a common templated-mesophase pathway, and possess a common stoichiometry. The solid derivative $[(\text{CdSe})_{13}(n\text{-propylamine})_{13}]$ is readily prepared on the gram scale. Because $[(\text{CdSe})_{13}(\text{RNH}_2)_{13}]$ compounds are useful low-temperature precursors to crystalline CdSe quantum belts,¹⁵ and presumably other CdSe nanocrystals, and because ligand exchange in $[(\text{CdSe})_{13}(\text{RNH}_2)_{13}]$ occurs readily, we expect that $[(\text{CdSe})_{13}(n\text{-propylamine})_{13}]$ will prove to be a useful, isolable form of $(\text{CdSe})_{13}$.

Experimental structure determinations have not been completed for any magic-size CdSe nanocluster, including $(\text{CdSe})_{13}$. Indeed, no single- x , magic-size $(\text{CdSe})_x$ nanocluster had been isolated in purity until earlier this year.¹³ However, the structure of $(\text{CdSe})_{13}$ has been determined theoretically,⁹⁻¹² and the lowest-energy C_3 isomer found by Nguyen, Day, and Pachter is plotted in Figure 6.¹⁰ These researchers also found the ligated nanoclusters of the type $[(\text{CdSe})_x(n\text{-methylamine})_x]$ to be stable with one amine ligand datively bound to each Cd atom.¹⁰ The structure of $[(\text{CdSe})_{13}(n\text{-methylamine})_{13}]$ was not reported, the $(\text{CdSe})_{13}$ component of which may differ from that in Figure 6. Calculations of the structural and spectral properties of $[(\text{CdSe})_{13}(n\text{-methylamine})_{13}]$ are currently in progress.²³

We measured the diameter of the $(\text{CdSe})_{13}$ nanocluster in Figure 6 to be 0.78 nm using molecular-modeling software. This value is close to the inter-amine-head-group spacing (0.80 nm) determined by analysis of the low-angle XRD data for the as-synthesized, bundled $[(\text{CdSe})_{13}(\text{RNH}_2)_{13}]$ mesophases (see the Results section). The similarity of these values supports our claim that a single monolayer of $(\text{CdSe})_{13}$ nanoclusters lies in each inter-amine-head-group lamellar gallery.

The state of the magic-size CdSe nanocluster field may be compared to that of the carbon-fullerene field just prior to the reported isolation of C_{60} by Krätschmer and Huffman in 1990.²⁴ At that time, C_{60} had been characterized by mass spectrometry, its structure had been determined theoretically, and some of its spectroscopic properties were known. After pure C_{60} became available in gram quantities,²⁴ the carbon-fullerene field grew rapidly. Similarly, we propose that access to gram quantities of $[(\text{CdSe})_{13}(n\text{-propylamine})_{13}]$ should enable experimental structure determination, reactivity studies, and further determinations of the physical and spectroscopic properties of $(\text{CdSe})_{13}$.

Conclusion

A convenient chemical synthesis affords the four $[(\text{CdSe})_{13}(\text{RNH}_2)_{13}]$ derivatives ($R = n$ -propyl, n -pentyl, n -octyl, and oleyl). These are the first derivatives of magic-size CdSe nanoclusters to be isolated in purity. The results establish the derivatives to have a common stoichiometry, and to have formed by a common amine-bilayer-template pathway. Remarkably, even the shorter-chain primary amines are able to generate amine-bilayer templates, which ultimately afford the $[(\text{CdSe})_{13}(\text{RNH}_2)_{13}]$ products in mesophase architectures. The diffraction data collected from the $[(\text{CdSe})_{13}(\text{RNH}_2)_{13}]$ mesophases allowed the first experimental estimate of the diameter of the $(\text{CdSe})_{13}$ nanocluster (0.80 nm), which is close to the theoretical diameter. Access to gram quantities of $(\text{CdSe})_{13}$ will enable further experimental studies.

Supplementary Material

Refer to Web version on PubMed Central for supplementary material.

Acknowledgments

This work was supported by the NSF under grant CHE-1012898 (to W.E.B.) and grants from the National Center for Research Resources (5P41RR000954-35) and the National Institute of General Medical Sciences (8 P41 GM103422-35) from the National Institutes of Health (to H.W.R.). We thank Ruth Pachter and Kiet A. Nguyen (Air Force Research Laboratory, Wright-Patterson Air Force Base, Dayton, Ohio) for providing the coordinates of $(\text{CdSe})_{13}$, and for sharing information prior to publication. We also thank Fudong Wang (Washington University) for helpful discussions.

References

- (1). Fojtik A, Weller H, Koch U, Henglein A. *Ber.Bunsenges. Phys. Chem.* 1984; 88:969.
- (2). Peng ZA, Peng XG. *J. Am. Chem. Soc.* 2002; 124:3343. [PubMed: 11916419]
- (3). Soloviev VN, Eichhofer A, Fenske D, Banin U. *J. Am. Chem. Soc.* 2001; 123:2354. [PubMed: 11456885]
- (4). Cumberland SL, Hanif KM, Javier A, Khitrov GA, Strouse GF, Woessner M, Yun CS. *Chem. Mater.* 2002; 14:1576.
- (5). Cossairt M, Owen JS. *Chem. Mater.* 2011; 23:3114.
- (6). Kudera S, Zanella M, Giannini C, Rizzo A, Li YQ, Gigli G, Cingolani R, Ciccarella G, Spahl W, Parak WJ, Manna L. 2006; 19:548.
- (7). Kui Y. *Adv.Mater.* 2012; 24:1123. [PubMed: 22432157]

- (8). Noda Y, Maekawa H, Kasuya A. *Eur. Phys. J. D.* 2010; 57:43.
- (9). Ben MD, Havenith RWA, Broer R, Stener M. *J. Phys. Chem. C.* 2011; 115:16782.
- (10). Nguyem KA, Day PN, Pachter R. *J. Phys. Chem. C.* 2010; 114
- (11). Singh T, Mountziaris T. J., Maroudas, D. *Appl. Phys. Lett.* 2012; 100:053105.
- (12). Kasuya A, Sivamohan R, Barnakov YA, Dmitruk IM, Nirasawa T, Romanyuk VR, Kumar V, Mamykin SV, Tohji K, Jeyadevan B, Shinoda K, Kudo T, Terasaki O, Liu Z, Belosludov RV, Sundararajan V, Kawazoe Y. *Nat. Mater.* 2004; 3:99. [PubMed: 14743211]
- (13). Wang YY, Liu YH, Zhang Y, Wang FD, Kowalski PJ, Rohrs HW, Loomis RA, Gross ML, Buhro WE. *Angew. Chem., Int. Ed.* 2012; 51:6154.
- (14). Dukes AD III, McBride JR, Rosenthal SJ. *Chem. Mater.* 2010; 22:6402.
- (15). Liu YH, Wang FD, Wang YY, Gibbons PC, Buhro WE. *J. Am. Chem. Soc.* 2011; 133:17005. [PubMed: 21905688]
- (16). Liu YH, Wayman VL, Gibbons PC, Loomis RA, Buhro WE. *Nano. Lett.* 2010; 10:352. [PubMed: 20014799]
- (17). Yener DO, Sindel J, Randall CA, Adair JH. *Langmuir.* 2002; 18:8692.
- (18). Evans CM, Love AM, Weiss EA. *J. Am. Chem. Soc.* 2012; 134:17298. [PubMed: 23009216]
- (19). Lambert, JB.; Shurvell, HF.; Verbit, L.; Cooks, RG.; Stout, GH. *Organic Structural Analysis.* Macmillan Publishing Co.,Inc.; New York: 1976.
- (20). Cossairt BM, Juhas P, Billinge SL, Owen JS. *J. Phys. Chem. Lett.* 2011; 2:3075. [PubMed: 22229074]
- (21). Ikawa N, O. Y, Kimura T. *J. Mater. Sci.* 2008; 43:4198.
- (22). Kitaigorodsky, AI. *Molecular crystals and molecules.* Academic Press; New York: 1973.
- (23). Pachter, R.; Nguyen, KA. personal communication
- (24). Kräetschmer W, Lamb LD, Fostiropoulos K, Huffman DR. *Nature.* 1990; 347:354.

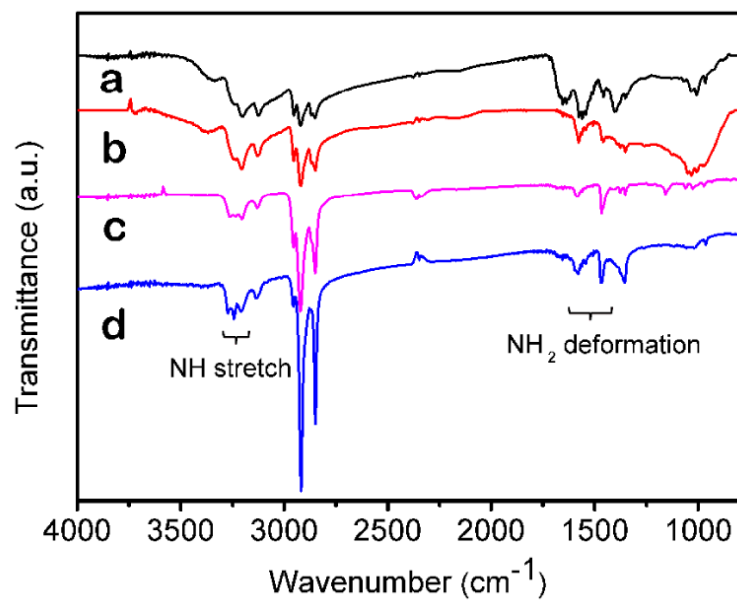


Figure 1. Infrared spectra (in KBr) of $[(\text{CdSe})_{13}(\text{RNH}_2)_{13}]$ complexes; R = *n*-propyl (a), *n*-pentyl (b), *n*-octyl (c), and oleyl (d). All absorbances were assigned to the amine ligands. Regions characteristic for NH stretching and NH₂ deformation are identified.

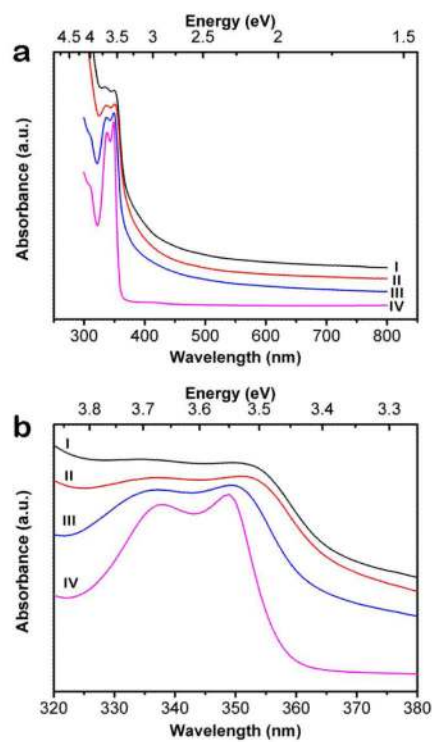


Figure 2. Absorption (extinction) spectra (in toluene dispersion) of $[(\text{CdSe})_{13}(\text{RNH}_2)_{13}]$ complexes; R = *n*-propyl (I), *n*-pentyl (II), *n*-octyl (III), and oleyl (IV). (a) full spectrum showing the characteristic absorbances of the $(\text{CdSe})_{13}$ nanocluster. Note the scattering tails in spectra I-III. (b) Spectral expansions in the region of the characteristic absorptions near 337 and 349 nm (see text).

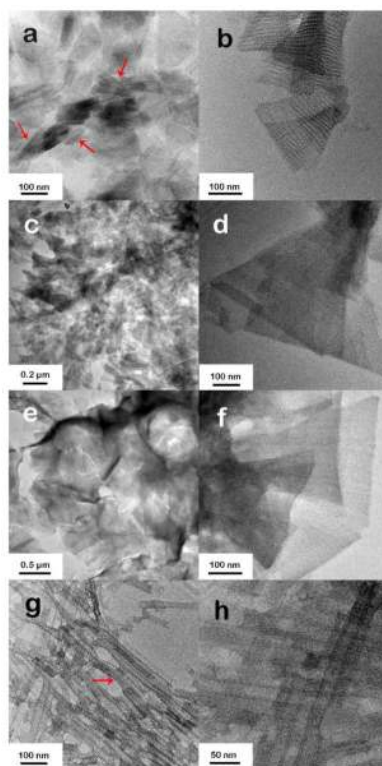


Figure 3. TEM images of the as-synthesized (bundled, left column) and unbundled (right column) $[(\text{CdSe})_{13}(\text{RNH}_2)_{13}]$; R = *n*-octyl (a, b), *n*-propyl (c, d), *n*-pentyl (e, f), and oleyl (g, h). The arrows in parts a and g identify bundled regions.

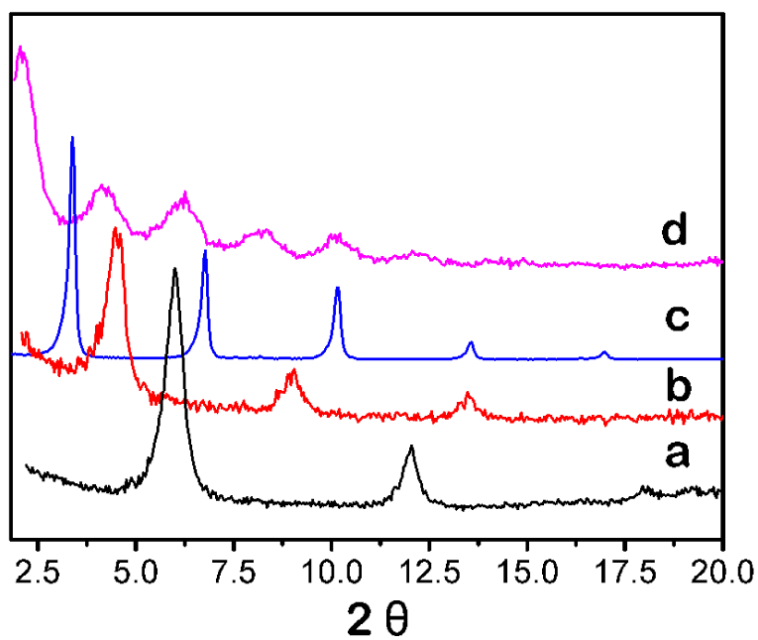


Figure 4. Low-angle XRD patterns of as-synthesized (bundled) $[(\text{CdSe})_{13}(\text{RNH}_2)_{13}]$ showing the basal reflections produced by the lamellar mesostructures; R = *n*-propyl (a), *n*-pentyl (b), *n*-octyl (c), and oleyl (d).

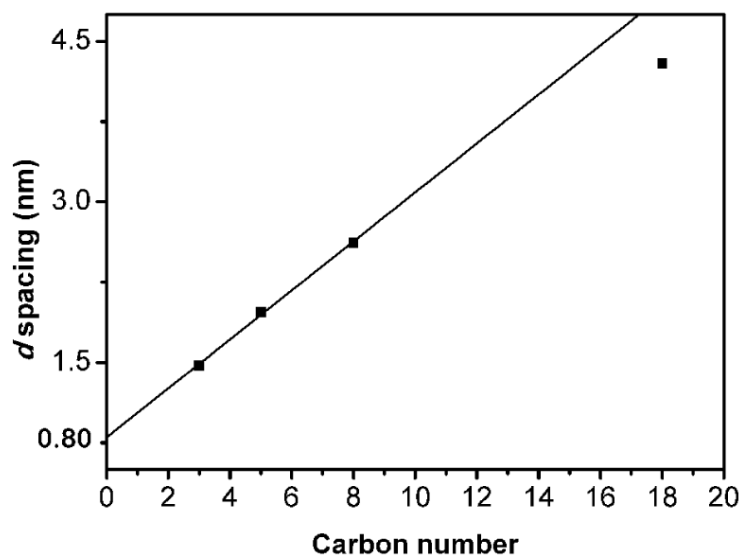


Figure 5. A plot of the measured basal-plane d spacing in the lamellar $[(\text{CdSe})_{13}(\text{RNH}_2)_{13}]$ mesostructures obtained from the XRD data versus the number of carbon atoms in the primary-amine ligands.

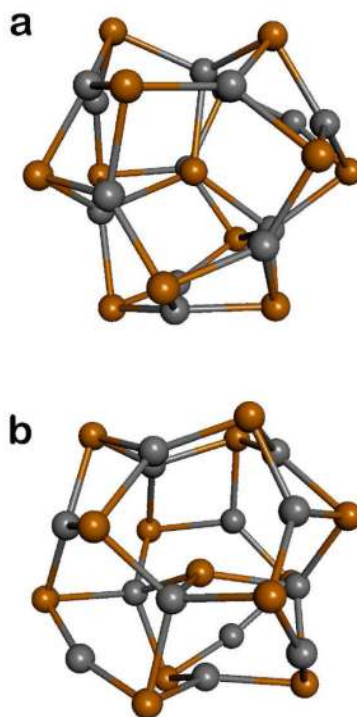
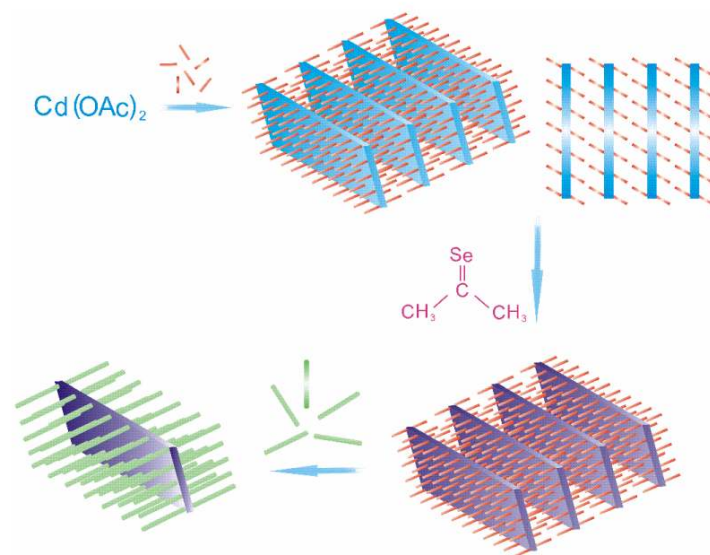


Figure 6. Two views of the lowest-energy isomer of unligated $(\text{CdSe})_{13}$ determined theoretically.⁶ The Cd atoms are gray, and the Se atoms are orange. (a) View with the C_3 axis perpendicular to the plane of the page; (b) view with the C_3 axis oriented vertically in the plane of the page. The plots were made using Accelrys Discovery Studio Visualizer.

**Scheme 1.**

Templated chemical pathway for the synthesis of $[(\text{CdSe})_{13}(\text{RNH}_2)_{13}]$ ^{13,15}. Combination of $\text{Cd}(\text{OAc})_2$ and the primary amine solvent forms a lamellar, bilayer template structure (blue, orange). Addition of selenourea results in the growth of $[(\text{CdSe})_{13}(\text{RNH}_2)_{13}]$ nanoclusters within the planar galleries of the template (purple, orange). Ligand exchange with oleylamine liberates sheet-like aggregates of $[(\text{CdSe})_{13}(\text{RNH}_2)_{13}]$ (purple, green) from the bundled template.

Table 1

Experimental (Exp) and calculated (Calcd) XRD basal-reflection positions in $[(\text{CdSe})_{13}(\text{RNH}_2)_{13}]$ compounds.

<i>00l</i>	$[(\text{CdSe})_{13}$ (oleylamine) ₁₃]	$[(\text{CdSe})_{13}$ (<i>n</i> -octylamine) ₁₃]	$[(\text{CdSe})_{13}$ (<i>n</i> -pentylamine) ₁₃]	$[(\text{CdSe})_{13}$ (<i>n</i> -propylamine) ₁₃]
	Exp, °2θ (Calcd, °2θ)	Exp, °2θ (Calcd, °2θ)	Exp, °2θ (Calcd, °2θ)	Exp, °2θ (Calcd, °2θ)
001	2.06	3.38	4.48	6.00
002	4.14 (4.12)	6.78 (6.76)	9.04 (8.96)	12.0 (12.0)
003	6.26 (6.18)	10.2 (10.1)	13.5 (13.4)	18.1 (18.0)
004	8.34 (8.24)	13.6 (13.5)		
005	10.2 (10.3)	17.0 (16.9)		
006	12.3 (12.4)			